Chemical Engineering Journal 427 (2022) 131885

Contents lists available at ScienceDirect

Chemical Engineering Journal

journal homepage: www.elsevier.com/locate/cej

Biofilm matrix and artificial mediator for efficient electron transport in CO_2 microbial electrosynthesis

Young Eun Song [a,b], Abdelrhman Mohamed [c], Changman Kim [b], Minsoo Kim [a], Shuwei Li [a], Eric Sundstrom [b], Haluk Beyenal [c,*], Jung Rae Kim [a,*]

[a] School of Chemical Engineering, Pusan National University, Geumjeong-Gu, Busan 46241, Republic of Korea
[b] Advanced Biofuel and Bioproducts Process Development Unit, Lawrence Berkeley National Laboratory, Emeryville, CA 94608, USA
[c] The Gene and Linda Voiland School of Chemical Engineering and Bioengineering, Washington State University, Pullman, WA 99164, USA

ARTICLE INFO

Keywords:
Microbial CO_2 electrosynthesis
Electron mediator
Bioelectrochemical system
Biofilms
Planktonic cell
HNQ

ABSTRACT

Microbial electrosynthesis (MES) has been highlighted as a means to valorize inorganic gaseous carbon, such as CO_2, into value-added chemicals using electricity as the reducing power. Electrode-based electron transfer delivers respiratory electrons to a live-cell biocatalyst through a biofilm matrix or via electron shuttle molecules. The addition of artificial mediators, such as neutral red (NR) and 2-hydroxy-1,4-naphthoquinone (HNQ), increased acetate synthesis significantly, suggesting that these mediators improve the electron transport capability between the suspended cells and electrode. Regular media replacement also improves MES by adapting mediator-utilizing species in the reactor. MES without a mediator initially produced acetate at a reasonable rate (5.1 ± 0.2 mmol/l/day), but the rate became negligible in the later stage. In contrast, MES with NR or HNQ showed a higher acetate production rate (4.6 ± 0.4 vs. 7.4 ± 0.4 mmol/l/day, respectively) as the media replacement progressed. Confocal laser scanning microscopy and 3D imaging showed that the biofilm matrix consisted of live and dead cells, while the composition was different in the MES with and without a mediator. Microbial community analysis by next-generation sequencing (NGS) showed that acetogenic *Acetobacterium* (in suspension) and *Sporomusa* (in both suspension and biofilm) were dominant during the 96 days of operation. The biofilm and planktonic community interacted dynamically under MES conditions. This result provides a realistic model of biofilms and planktonic cells in the MES. The interaction of the suspended cells with the biofilm-forming electrode via electron shuttles could improve volumetric acetate production and stabilize the MES performance.

1. Introduction

Global greenhouse gas emissions were estimated to be 3.4×10^4 million tons in 2019 and increased steadily by 1.1% from 2008 to 2018 [1]. These emissions are expected to grow more rapidly in non-OECD countries because of population and economic expansion. Beyond emission reductions, the reutilization and valorization of CO_2 have attracted considerable research attention internationally. CO_2 is the most oxidized form of carbon in nature. Hence, to convert CO_2 to value-added chemicals, a suitable strategy for reducing CO_2 is in strong demand [2,3].

Microbial electrosynthesis (MES) has attracted considerable interest as a prospective route for providing large amounts of reducing equivalents for sustainable CO_2 conversion using renewable electricity [4–8]. MES uses an electrode as an electron donor to convert CO_2 to C1 to C5 compounds using various electroactive microbes [9–11]. Such live-cell biocatalysts have the advantages of cost-effectiveness, high specificity, operation at room temperature and pressure, and self-replication. The electron delivery from the electrode to bacteria has been reported to use direct electron transport through the biofilm matrix [12–15] or indirect transfer via artificial or self-producing mediators, highlighting the need to investigate further improvements in the system performance [8,10,16]. Slow biofilm development on an electrode and low cell growth in suspension has frequently been highlighted as problems in

Abbreviations: MES, Microbial electrosynthesis; NR, Neutral Red; HNQ, 2-hydroxy-1,4-naphthoquinone; OC, No mediator open circuit; MES, MES without a mediator; MES-NR, MES with NR; MES-HNQ, MES with HNQ.

* Corresponding authors.
E-mail addresses: beyenal@wsu.edu (H. Beyenal), j.kim@pusan.ac.kr (J.R. Kim).

https://doi.org/10.1016/j.cej.2021.131885

Available online 21 August 2021

autotrophic CO_2 conversion, such as MES [11,17]. Furthermore, the electrosynthetic biofilm and its interactions with suspended bacteria during operation have not been studied extensively [18–20].

The direct electron transfer (DET) exchanges respiratory electrons between the microbes and solid electrodes without shuttle molecules. Biofilm developments on the carbon electrode and corrosive metal surfaces have been reported [21,22]. Most studies on MES focused on the structural design/fabrication and surface modification of the electrode material for efficient electron transfer for CO_2 reduction [23–25]. Jourdin et al. reported a macroporous reticulated vitreous carbon electrode to enhance electrosynthesis [26]. They achieved the higher specific acetate production of 1330 g/m^2·d with biofilm formation. Alqahtani et al. developed a porous hollow fiber nickel electrode to enrich the methanogenic community on the electrode surface and obtained higher methane conversion with a faradaic efficiency of up to 77% [27]. On the other hand, electrode surface area-dependent bioconversion like MES still has the drawbacks of a low volumetric production rate and titer and stability. Recently, some research groups reported stable MES performance against power supply interruption and influent CO_2 flow fluctuation [7,28]. Nevertheless, these drawbacks need to be resolved before industrial and field-scale applications can be achieved [8].

Indirect electron transfer (IET) delivers electrons through electroactive shuttle molecules or generated H_2 [8,29,30]. Seelajaroen et al. reported that *Methylobacterium extorquens* biofilms catalyzed the electrochemical reduction of CO_2 to formate [31]. They showed that the redox mediator (i.e., neutral red) enhanced formate production and the faradaic efficiency of the cells. Such a mediator also improved electrosynthetic CO_2 conversion to organic acids in a batch operation. Bajracharya et al. reported that the acetate production rate decreased when MES operation was switched from batch to continuous mode [32], probably due to the washout of planktonic cells. On the other hand, the performance was recovered when the operation was returned to batch mode. These results suggest that the suspended cells may be more active in MES over the electrode-attached (biofilm-forming) community.

The interactions of biofilms and planktonic cells are essential for understanding the mechanism and improving the MES performance [5,11]. The applied potential and current flow to the cathode are expected to influence biofilm formation and attract (or repel) planktonic cells [33]. On the other hand, protons can be reduced to hydrogen at potentials more negative than −630 mV vs. Ag/AgCl (3 M KCl, pH 7) in MES. Therefore, the abiotically produced H_2 molecule can act as an electron shuttle between the electrodes and cells [34]. These parameters and conditions of MES may dynamically regulate the composition of the community in both biofilms and suspensions.

Most MES studies focused on the biocathode (i.e., electrode-associated biofilm through direct electron transfer). In contrast, there is limited knowledge of MES operated with suspended culture and the role of the electron transfer mediators and shuttle molecules. The morphology and electrochemical characteristics of electrosynthetic biofilms, and their changes over long-term operation have not been well studied. The delivery of electrons to the suspended microbes and the electrode-associated biofilm is essential for increasing the volumetric production of target metabolites in a scale-up process.

This study compared the performance of MES and the shift in the microbial community when different electron transfer mediators are used. The culture media was replenished periodically to remove the suspended bacteria but maintain the electrode-associated electrosynthetic biofilm. Such replacement of culture enhanced acetate production from CO_2 using neutral red (NR) and 2-hydroxy-1,4-naphthoquinone (HNQ) as the electron mediator. The performance of MES was evaluated by examining the electrochemical analysis and morphological characteristics of biofilms by cyclic voltammetry (CV), electrochemical impedance spectroscopy (EIS), and confocal laser scanning microscopy (CLSM). The microbial community was analyzed by next-generation metagenome sequencing. Although further biological and morphological analyses are required, this work provides a realistic model of the interactions of biofilm and planktonic community in MES in the presence of electron transfer mediators. The combination of mediator-based and electrode-associated MES could improve volumetric acetate production in such electrode-based bioconversion.

2. Material and methods

2.1. Reactor configuration and culture media

H-type two-chamber bioelectrochemical systems (BES) were used for microbial CO_2 electrosynthesis (in cathode) and water electrolysis to produce electron and proton (in the anode) (See details in Supplementary Information 1 and Fig. S5) [5]. The bacterial media contained the following: KH_2PO_4, 3.0 g/L; K_2HPO_4, 5.8 g/L; $NaHCO_3$, 4 g/L; NH_4Cl, 0.5 g/L; $MgCl_2{\cdot}6H_2O$, 0.09 g/L; $CaCl_2{\cdot}2H_2O$, 0.0225 g/L; yeast extract, 0.5 g/L; 20 ml of designed Pfennig's trace metal and vitamin solutions [35]. No carbon sources other than CO_2 were used in the culture of MES. 2-Bromoethanesulfonate (BES, 5 mM) was added to the media to prevent methanogenic activity. The anode chamber was filled with the same media (250 ml) except for the yeast extract. The cathodic pH was titrated to pH 7, and the anodic pH was regulated to pH 2 by HCl. In some experiments, the electron mediators (0.5 mM), 2-hydroxy-1,4-naphthoquinone (HNQ) or neutral red (NR) were added to facilitate electron transfer between the microbe and electrode in the cathode chamber.

2.2. Operation of MES reactor

The cathode chamber (working volume of 250 ml) was inoculated with 25 ml of secondary anaerobic digestion sludge obtained from the Pullman Wastewater Treatment Plant in WA, USA. During operation, the culture broth was replaced periodically with fresh medium (80%) at the end of each phase (P1 to P4). The filtered CO_2 feed gas (99.9%, v/v) was introduced to the bottom of the cathode chamber side arms through a needle with a 40 ml/min flow rate. The anode chamber was purged with N_2 gas (99.9%, v/v) at 50 ml/min to remove the oxygen produced from water electrolysis. The feed gases were passed through the oxygen trap manufactured using copper granules and a heating mantle (300 °C) to eliminate trace oxygen from the gas cylinder.

For the cathodic electrosynthesis of CO_2, an applied potential at −1.11 V (vs. Ag/AgCl 3 M KCl) was applied continuously to the cathode electrode (i.e., working electrode) by chronoamperometry using a multichannel potentiostat (32 channels, WBCS3000LEe32, WonA Tech, Korea). The open-circuit reactor (OC) was operated without externally poised potential. Thus, the cathode electrode of OC does not act as an electron donor. All reactors were located in a thermostatic room at 30 ± 1 °C.

2.3. Electrochemical analyses

The electrochemical characteristics of the biofilm-forming cathode were examined by cyclic voltammetry (CV) and electrochemical impedance spectroscopy (EIS) using a potentiostat (Versastat 3, Ametek, USA) with Versa Studio™ software. CV was conducted at a scan rate of 10 mV/s with a scan range between −1.5 and 0.5 V versus the reference electrode. EIS was carried out over the frequency range of 0.1 Hz–500 kHz and a sinusoidal perturbation amplitude of 5 mV. The coulombic efficiency, ratio of electrons (in coulombs) consumed by electrode-based CO_2 synthesis, and the electrons recovered by the product (acetate) were calculated using the following equations:

$$2CO_2 + 8H^+ + 8e^- \rightarrow CH_3COOH + 2H_2O \quad (1)$$

$$C_p(\mathrm{C}) = n \times F \times m \quad (2)$$

$$C_E(\mathrm{C}) = \int_0^t Idt \tag{3}$$

$$CE = C_P / C_E \times 100 \tag{4}$$

where n, F, m, and I (C/s) denote the moles of recovered electrons in the product (i.e., acetate; eight moles of e^-), Faraday's constant (96,485 C/mole of e^-), acetate produced during operation from time 0 to t, and the current recorded by the potentiostat, respectively. The coulombic efficiency (CE) of electrosynthesis was calculated using Eq. (4).

2.4. Analyses of the metabolites and biofilm morphology

The liquid samples were collected periodically and centrifuged at 5000 rpm for 5 min. The supernatants were filtered through a syringe filter (Nylon22LN13MT, 13 mm diameter, 0.22 μm pore size, Aura Industries Inc., USA). The filtered samples were analyzed by high-performance liquid chromatography (HPLC, HP 1160 series, Agilent Technology, USA) equipped with a 300×7.8 mm Aminex HPX-87H (Bio-Rad, USA) column at 65 °C and refractive index (RI) and photodiode array (PDA) detector using 2.5 mM of H_2SO_4 as the mobile phase (flow rate = 0.5 ml/s). The volatile fatty acids (VFAs) in the samples were analyzed by gas chromatography (GC, 7890B, Agilent Technology, USA) equipped with a flame ionization detector (FID) and an HP-FFAP column (Agilent, USA) with helium (1 ml/min) as the carrier gas. The detector and injector temperatures were 300 °C and 250 °C, respectively. The oven temperature was started at 60 °C for 10 min and increased to 80 °C at 20 °C/min. The temperature was then increased to 170 °C at 10 °C/min and held at that temperature for 6 min. The oven temperature was increased to 240 °C at 80 °C/min and held at that temperature for 5 min. The turbidity of the suspension was determined from the optical density using a UV-visible spectrophotometer (Optizen POP, Mecasys Co. Ltd. South Korea) at 600 nm (OD600). The pH was analyzed using a pH meter (Orion 420A+, Thermo, USA).

Spectral imaging confocal laser scanning microscopy (LSM 800, ZEISS, Germany) was carried out to examine the morphology of biofilm-covered electrodes. At the end of the experiment, 1 × 1 cm^2 of the electrode samples were taken from the reactor. The electrodes were washed with a growth medium and stained with propidium iodide and SYTO 9 using a LIVE/DEAD BacLight bacterial viability kit (L10316, Invitrogen Corp., Carlsbad, CA). The stained electrodes were placed on microscope slides with coverslips elevated above the electrode thickness and viewed using 482-nm and 635-nm lasers (See details in Supplementary Information 2) [36].

2.5. Analysis of bacterial community using metagenome sequencing

At the end of the experiment (at 96 days of operation), the bacterial DNA samples from the biofilm on the cathode electrode and planktonic cells in the catholyte were characterized by next-generation sequencing (NGS, Macrogen, Korea). For more specific sample treatment and amplification, see Supplementary Information 3.

3. Results and discussion

3.1. Microbial electrosynthesis of CO_2 without a mediator

3.1.1. Comparison of acetate production in open and closed circuit MES

Acetate production in an open (OC) and closed-circuit MES without a mediator (hereinafter called MES) were examined with periodical media replacement. During the first 25 days (Phase 1), the acetate production level and rate obtained were up to 126.3 ± 3.9 mM and 5.1 ± 0.2 mM/day (7.5 g/L and 0.30 g/L/d), respectively (Fig. 1a), but it showed a remarkable decrease after media replenishment from Phase 2 (with 80%

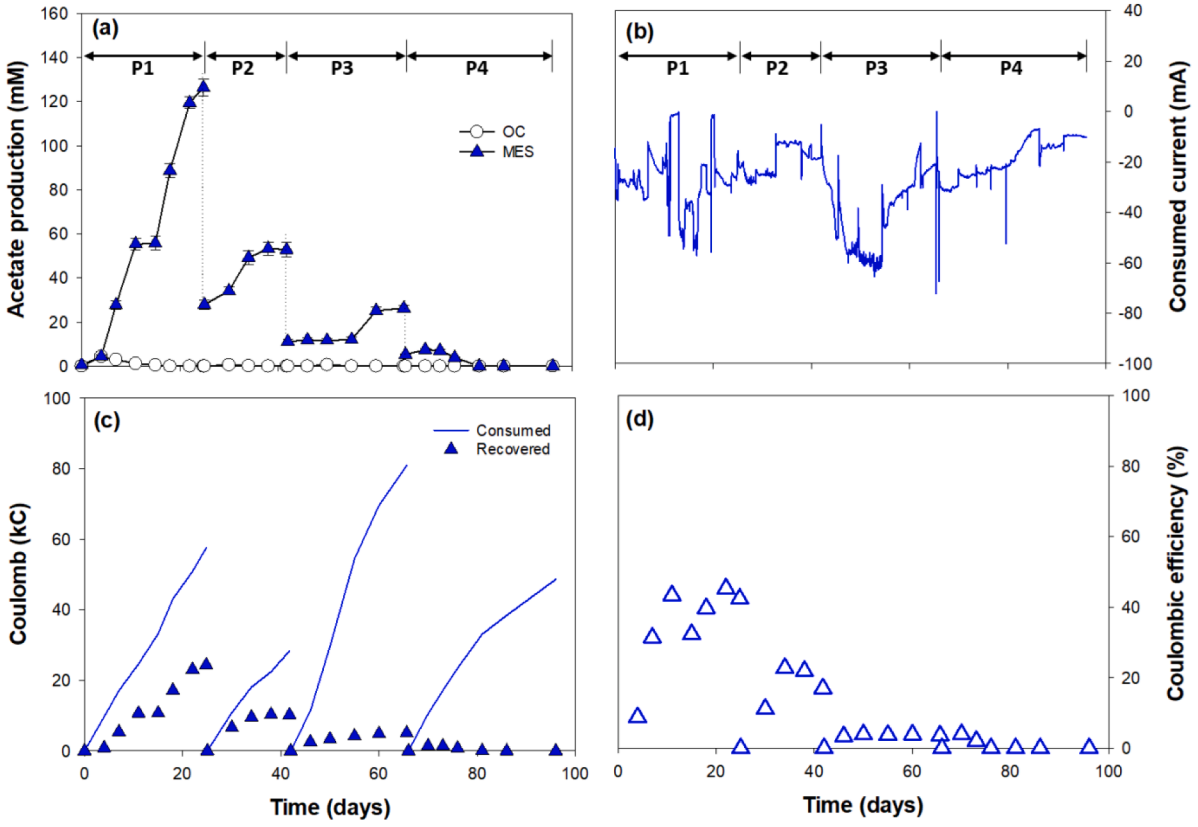

Fig. 1. Acetate production of open circuit (OC) and MES without a mediator (MES). (a) acetate production, (b) current consumption, (c) coulomb consumed and recovered into acetate, (d) coulombic efficiency. P1–P4 indicate each phase with media replacement.

media replaced in each phase). In Phases 2 and 3, only 25.0 ± 3.4 and 15.1 ± 1.6 mM of acetate, respectively, were produced, and none was detected at the end of Phase 4. In the OC, in which no electrons were provided, acetate production was below 4.5 mM in the early stages of Phase 1, and negligible amounts were produced thereafter. This result suggests that the electrode-based electron transfer facilitates CO_2 reduction to acetate compared to the OC condition (i.e., without an additional electron source). The cathodic electrosynthesis with CO_2 continuously consumed the protons and electrons that migrated from anodic water electrolysis in a closed-circuit MES (see the schematic diagram of MES in Supplementary Information Fig. S5) [5]; thus, the anodic pH was continuously maintained at approximately pH 2 (Fig. S1b–d). The anodic pH in the OC increased at the end of the phases because the protons diffused to the cathode via the concentration gradient across the membrane, but no such water electrolysis occurred in the anode (Fig. S1a).

Fig. 1b–d shows the coulomb consumption and recovery of MES. The current consumed by the reactor was varied, and the average current density based on the electrode surface was approximately 14.5 A/m^2 (Fig. 1b). Fig. 1c gives the time course of the coulombs recovered to acetate. Coulomb consumption in the initial two phases was 57.6 and 28.4 kilo-coulombs (kC) with simultaneous acetate production. In the 3rd and 4th phases, however, coulomb consumption increased significantly to 80.1 and 48.6 kC, but only a small amount of acetate was produced. The maximum coulombic efficiency obtained was 45.3% in Phase 1, but it decreased significantly after serial media replacement (Fig. 1d).

These results suggest that MES proceeds mainly by the suspension or microbe "loosely" bound to the electrode. Therefore, it is easily washed out throughout the subcultivation. Thus, the recovery of electrons into acetate was significantly lower in the later stages with periodic media replacement. The leakage of electrons can occur through hydrogen without capturing CO_2 because the applied potential of −1.11 V vs. Ag/AgCl is sufficient to produce abiotic H_2 production. In previous reports, the switching of operation from batch to continuous mode decreased the acetate production rate in MES significantly [32]. In contrast, other studies reported that partial media replacement enhanced acetate production [7,37], probably by preventing acetate and other VFA accumulation and simultaneously providing fresh nutrients. On the other hand, the effects of media replacement and the involvement of electrode-associated biofilms in MES have not been discussed in previous studies. In MES, the negatively charged cathode electrode may act as a repulsive force for suspended cells [38]; hence an acetate producing biofilm may not be developed in the early phase (Phase I). The media replacement washed out the suspended cells; subsequently, acetate production decreased significantly in the following phases.

3.1.2. Morphology of associated biofilm on the electrode of MES

The morphology of the associated biofilm was analyzed by taking the electrode sample at the end of the experiment (96 days of operation under MES with CO_2) and observing them by confocal laser scanning microscopy (CLSM). Propidium iodide (green color) and SYTO 9 (red color) staining visualized the morphological distribution of live and dead cells on the electrode, respectively. Fig. 2 presents the fluorescent image with the thickness and cell viability. The cathodic biofilm from MES showed dense and homogeneously distributed live/dead cells with a thickness of up to 300 μm (Fig. 2b). In contrast, lower biomass with a relatively higher dead cell distribution (thickness of ~50–100 μm) was obtained from the OC (Fig. 2a). CLSM showed that the applied potential influences biofilm formation on the electrode in microbial electrosynthesis. Providing a reducing equivalent drives bacterial association to the electrode surface. Although the apparent biofilm was obtained from MES, periodic media replacement may deteriorate the performance of acetate electrosynthesis by removing the suspended bacteria, as shown in Fig. 1a.

3.1.3. Electrochemical characteristics of OC and MES

The mechanism of the electrochemical properties of the biofunctionalized cathode was analyzed by CV and EIS in the middle of each phase. CV indicated electron transfer between the electron donor (i.e., solid carbon felt) and acceptor (i.e., CO_2) through biofilm and the mediator. The redox peaks were shifted slightly from the standard reduction potential under MES conditions (Fig. 3c). The reduction peaks appeared at approximately −430 and −620 mV vs. Ag/Cl, which were likely to be associated with acetate and hydrogen production via direct electron transfer from the electrode [5,16].

Acetate production from CO_2 reduction is related to the first reduction peak at approximately −430 mV vs. Ag/AgCl; it appeared from Phase 1 with a peak current of 12 mA, but the peak disappeared from Phase 2. The CV peak at approximately −620 mV vs. Ag/AgCl is probably related to hydrogen evolution and was observed from Phase 2. In contrast, the OC showed a much lower redox capability and electrical capacitance even after inoculation and throughout the phases with no acetate detected (Fig. 1a and Fig. 3a).

EIS evaluates the electron transfer resistance between the biofilm and cathode electrode and the diffusion resistance of the biofilm surface and electrolyte interface. Fig. 3b and d presented Nyquist plots of the OC and the MES, respectively. The circuit model of MES consisted of an ohmic resistance (R_Ω), charge transfer resistance (R_{ct}), and a constant phase element (CPE), as shown in Fig. 3e. The R_Ω is the faradaic component related to the resistance caused by the bacterial media, ion exchange membrane, and reactor configurations. R_{ct} is the faradaic component that arises from the interface between the electrode surface

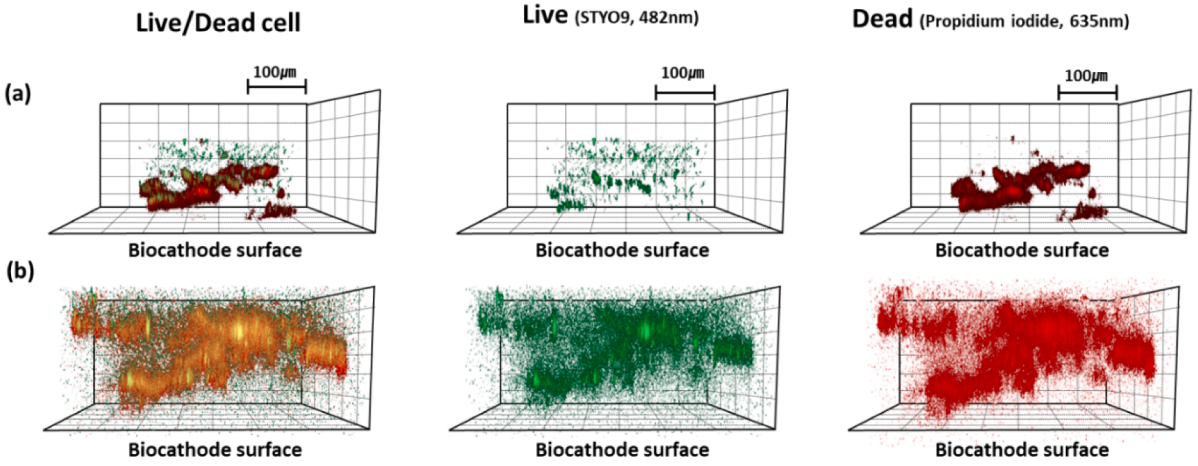

Fig. 2. Live and dead cell distribution within the biofilm on the electrode was analyzed by CLSM. (a) OC, and (b) MES.

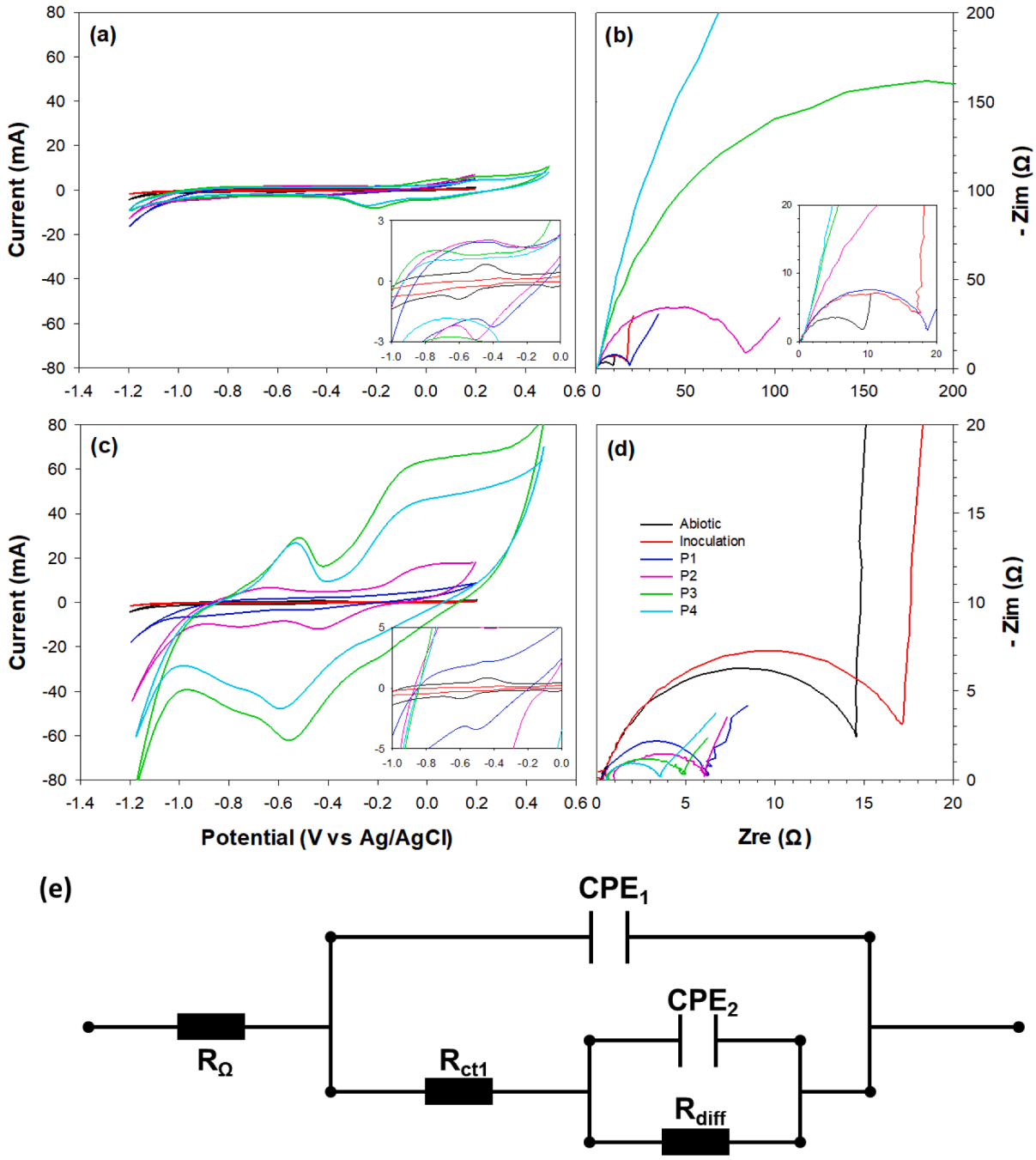

Fig. 3. Cyclic voltammetry (CV) and electrochemical impedance spectroscopy (EIS) of OC and MES without a mediator. CV and EIS were carried out in the middle of each phase. (a) & (b) OC, (c) & (d) MES, (e) Electrochemical circuit model of MES.

and the surrounding electrolyte. In contrast, the CPE is a non-faradaic component representing the double layer capacitance resulting from the rough and porous structure of the electrode. The R_{Ω}s were estimated to be below 1.0 Ω in the OC and MES, measured from zero to the start point of the first semicircles. The first semicircles obtained at a high-frequency range are related directly to interfacial charge transfer resistance between the electrode and biofilms [39]. The charge transfer resistance increased in OC (from 18.7 to 953.3 Ω) while it decreased slightly in MES (from 5.9 to 3.2 Ω) during the four-phase operation (Table 2). The diffusion resistance (R_{diff}) indicated the 2nd semicircles at a low-frequency range, which are related to interfacial charge transfer resistance between the biofilm (or electrode) and other electron acceptors in the suspension, such as protons or electron mediator. R_{diff} decreased gradually after media replacement throughout the phases, indicating that electron transfer to the suspension had been facilitated. On the other hand, without a mediator, these electrons may result in proton reduction to H_2 rather than electrosynthesis, considering the CV and less acetate production.

3.2. Microbial electrosynthesis in MES with neutral red (NR)

3.2.1. Acetate production and biofilm morphology in NR-fed MES

Neutral red (NR) has a similar standard reduction potential to the NADH/NAD^+ couple (−535 mV vs. −530 mV Ag/AgCl) and undergoes a two-electron reduction/oxidation process. NR binds to the cell membrane easily and is less toxic [5,40]. The reduced NR acts as an electron donor to influence cell growth and the metabolism in microbial fermentation by generating a proton motive force [41–43]. NR was also

reported to enhance the production of volatile fatty acids (VFAs) as an electron donor in electrosynthesis and electro-fermentation [6,31,40,43–46].

Fig. 4a and b present the level of acetate production of NR-fed MES (MES-NR) and current consumption. The consumed current showed fluctuated in Phase 1, then stabilized with a current density of approximately 3.4 A/m^2 from Phase 2 (Fig. 4b). Acetate production increased gradually in each phase from 74.3 ± 7.6 (Phase 1) to 137.5 ± 0.3 mM (Phase 4). The estimated production rates in Phases 1 and 2 were 3.0 ± 0.4 and 2.8 ± 0.6 mM/day, respectively, but they increased significantly to 3.4 ± 0.5 and 4.6 ± 0.4 mM/day (0.40 and 0.26 g/L/d, respectively) in Phases 3 and 4, respectively. The coulombs consumed decreased gradually from 58.7 to 33.0 kC, while the recovered coulombs into acetate increased (Fig. 4c). Therefore, the coulombic efficiencies in each stage increased to the final CE of 86.9% in Phase 4 (Fig. 4d). The CLSM image of MES-NR indicates that a 50–100 μm thick biofilm contains many more dead cells (Fig. 4e). The level of dead cells was similar to that of OC in Fig. 2a. Therefore, the CO_2 electrosynthesis of MES-NR appears to occur mainly in the suspended bacteria using NR as an electron shuttle rather than the electrode-associated biofilm.

The initial acetate production of MES-NR (Fig. 4a) was lower than MES without a mediator (Fig. 1a). On the other hand, continuous media replacement resulted in increasing acetate production and a higher CE. This suggests that the addition of NR exerts selective pressure on the bacterial community. Hence, the planktonic cells effectively utilize the cathode using NR as an electron shuttle. At Phase 4, the acetate titer achieved up to 8.1 ± 0.1 g/L, which was relatively higher than previous MES studies with CO_2 (Table. 2) [8]. Thus, the electron mediator appears to compensate for the limitation of the electrode surface area of MES by the effective and flexible delivery of electrons, providing a potential strategy for the volumetric scale-up of electrode-based bioconversion processes, such as MES.

3.2.2. *Electrochemical characteristics of MES-NR*

Adding NR resulted in a significant change in CV compared to OC and MES without a mediator (Fig. 5a). The abiotic control showed clear redox peaks, but they decreased when inoculated and throughout media replacement, probably due to adsorption and interactions with bacteria. The reduction peaks were also shifted slightly to a positive potential compared to those of the abiotic control. In contrast, the peak currents increased to −17 and −27 mA (Phase 4) in the first and second peaks, respectively (Fig. 5a). On the other hand, the increased oxidation peaks

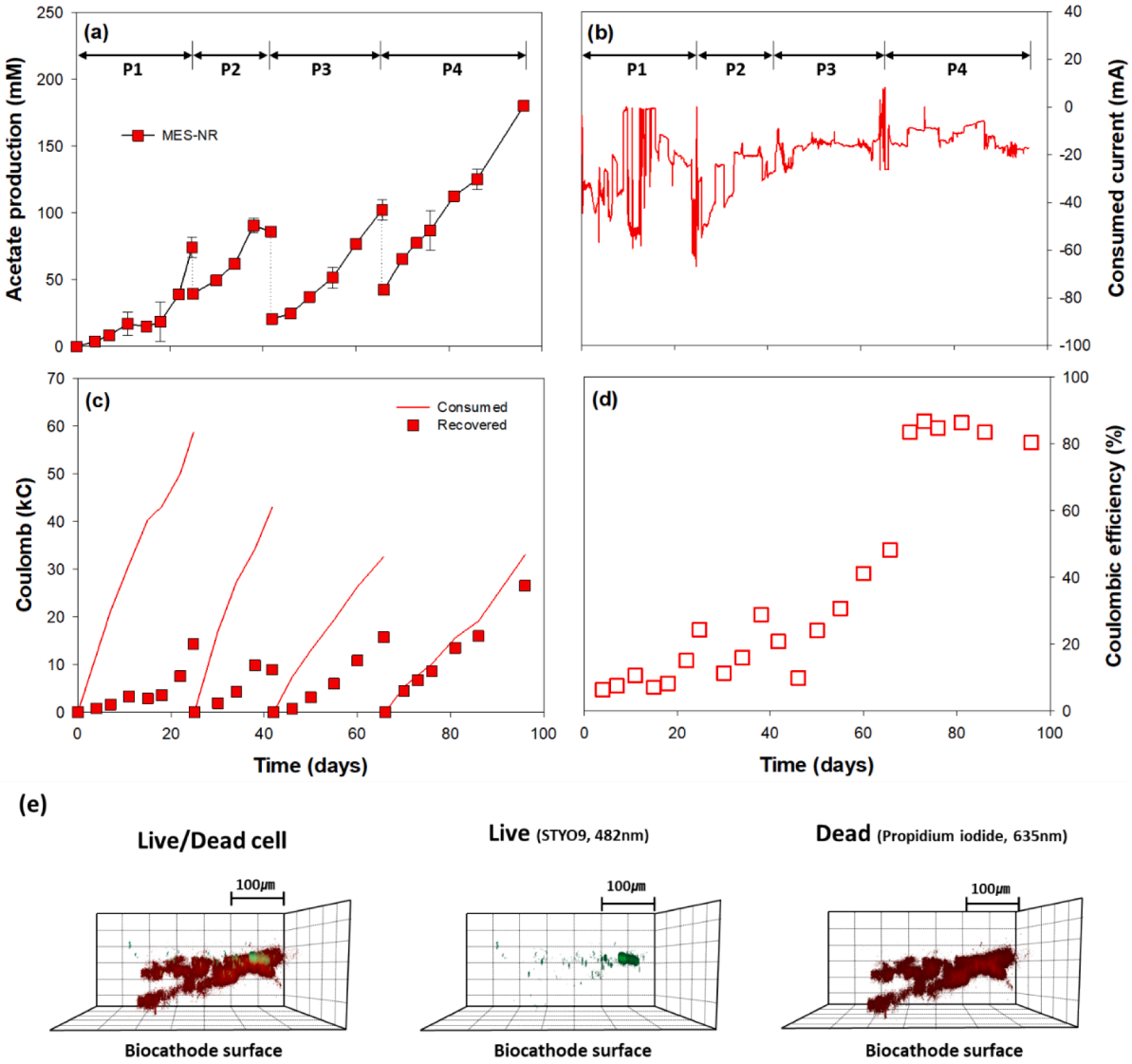

Fig. 4. Acetate production from neutral red-fed MES (MES-NR). (a) acetate production, (b) current consumption, (c) coulomb consumed and recovered into acetate, (d) coulombic efficiency, (e) The live and dead cell distribution within the biofilm on the electrode analyzed by CLSM image. P1–P4 indicate each phase with media replacement. (For interpretation of the references to color in this figure legend, the reader is referred to the web version of this article.)

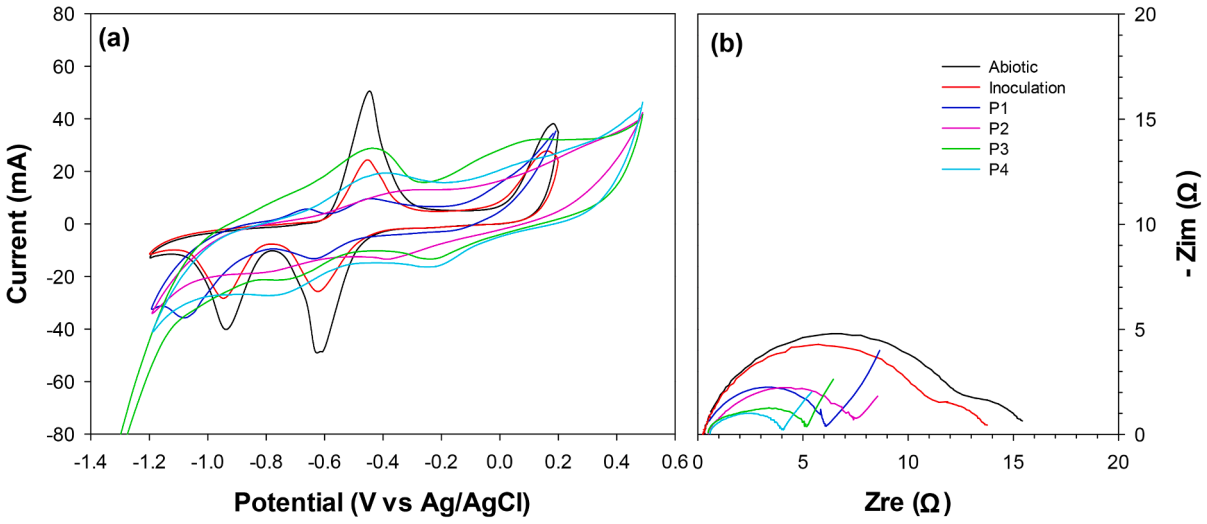

Fig. 5. (a) Cyclic voltammetry (CV) and (b) electrochemical impedance spectroscopy (EIS) of MES-NR. CV and EIS were carried out in the middle of each phase.

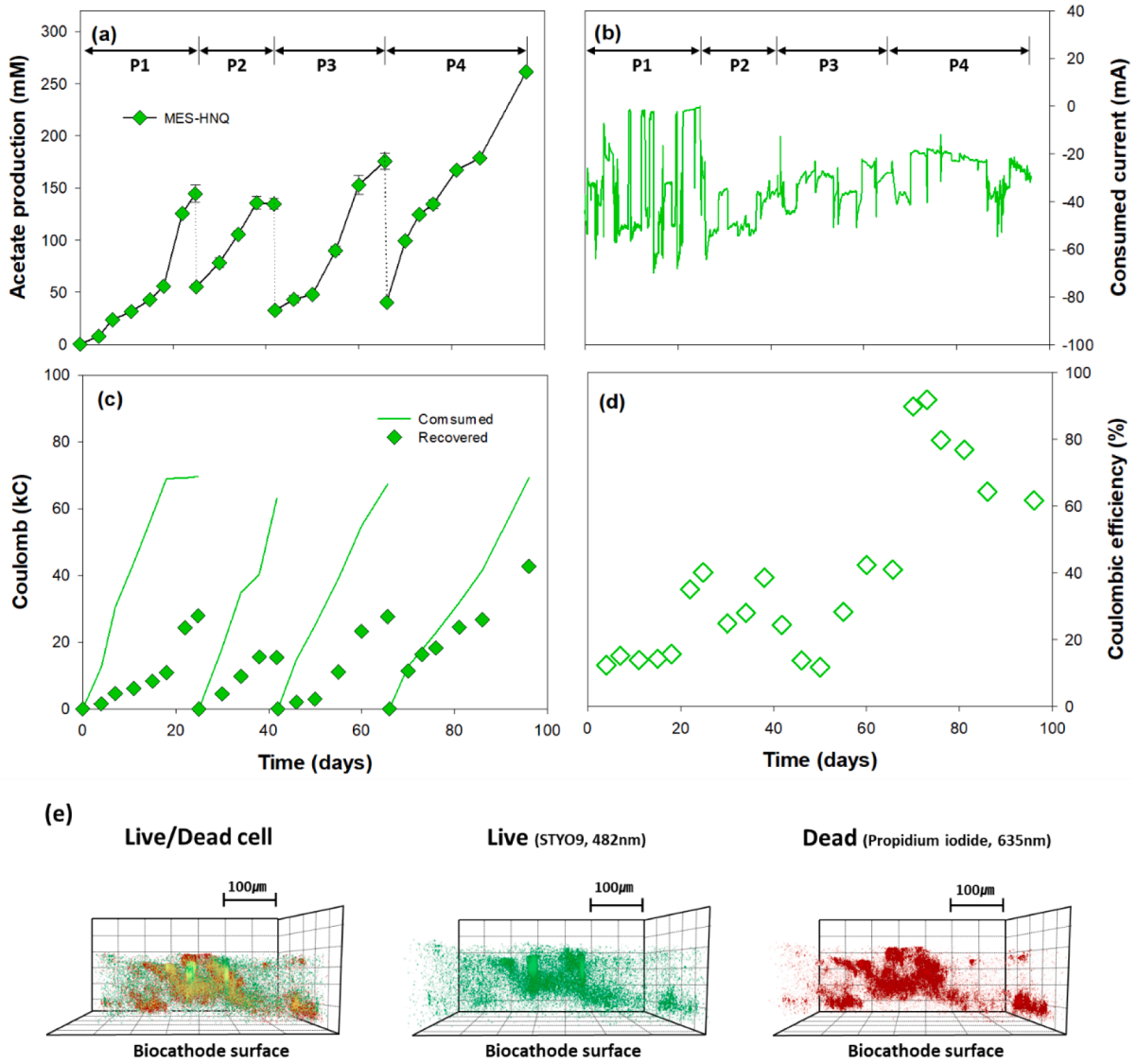

Fig. 6. Acetate production of HNQ-fed MES (MES-HNQ). (a) acetate production, (b) current consumption, (c) coulomb consumed and recovered into acetate, (d) coulombic efficiency, (e) The live and dead cell distribution within the biofilm on the electrode analyzed by CLSM. P1–P4 indicate each phase with media replacement.

from Phase 2 indicate that acetotrophic and other unknown microbes in suspension may consume the acetate produced from electrosynthesis. Although the redox peaks of CV were not defined and explained clearly, the apparent acetate production at each phase (Fig. 4a) indicates NR augmentation and serial media replacements make the community more favorable for CO_2 electrosynthesis by transferring electrons from the electrode to bacteria effectively.

The R_Ω obtained from MES-NR were approximately 1 Ω, which is similar to the MES without a mediator. The 1st semicircle, the charge transfer resistance, decreased gradually from 5.6 (Phase 1) to 3.5 Ω (Phase 3) but increased slightly to 6.9 Ω at Phase 4. In contrast, the 2nd semicircle, the diffusion resistance, was lower than the charge transfer resistance at the initial stage but increased in the later stages due to biofilm formation from Phase 1 (Fig. 5b, Table 2).

3.3. Microbial electrosynthesis in MES with HNQ

3.3.1. Acetate production and biofilm morphology in HNQ-fed MES

Quinones act as electron carriers in many respiratory chains of living cells and are distributed widely in nature [47]. 2-Hydroxy-1,4-naphthoquinone (HNQ, called lawsone) is one of the simplest naturally occurring naphthoquinones and is easily transported through the cell membrane. HNQ has two non-sequential standard redox potentials, HNQ/HNQH and HNQH/$HNQH_2$ (−75 and −625 mV vs. Ag/AgCl, respectively); the 2nd reduction potential is below the NADH/NAD^+ couple (−530 mV vs. Ag/AgCl) [5]. HNQ experiences two successive one-electron reductions or a two-electron reduction depending on the conditions [48].

The MES-HNQ produced 144.5 ± 8.5 mM in Phase 1, which was slightly higher than those of MES and MES-NR (Fig. 6a). Current consumption ranged from 0 to −60 mA, but it stabilized between −20 and −40 mA from Phase 2. The current density based on the electrode surface area was 14.0 A/m^2 at Phase 1, then slightly decreased to 12.9 A/m^2 from Phase 2 (Fig. 6b). The acetate production rate increased gradually from 5.8 ± 0.6 (Phase 1) to 7.4 ± 0.4 mM/day (0.44 g/L/d) (Phase 4); the rates were 1.5 and 1.8 times higher than those of MES and MES-NR in all phases. The level of acetate production was up to 220.8 ± 2.5 mM, and the maximum coulombic efficiency reached 91.9 % in Phase 4 (Fig. 6c & d). The pH in the cathode chamber decreased to 5, indicating that the acetate was accumulated by electrosynthesis (Fig. S1d). The CLSM image of MES-HNQ presented homogeneously distributed live/dead cells within the biofilm (Fig. 6e). The thickness of the biofilm (~150 μm) was similar to that of MES-NR but had a higher live cell distribution than MES-NR within the biofilm. The developed biofilm appears to be resistant against washing out by serial media replacement and hence stabilize the electrosynthesis. As a result, MES-HNQ achieved a significantly higher acetate production titer of 13.3 ± 0.2 g/L than in the previous results (Table 1) [8].

3.3.2. Electrochemical properties on CO_2 electrosynthesis in MES-HNQ

The CV curve showed clear redox peaks of HNQ abiotically but was changed considerably after inoculation and MES operation. From Phase 1, the oxidation peak was shifted towards the negative direction, whereas the reduction peaks shifted to the positive direction, and the 1st and 2nd oxidation peaks increased appreciably from Phase 2. The electrical capacitance increased in the later phases, probably due to biofilm formation on the electrode (Fig. 7a). During CO_2 electrosynthesis, the redox peak was separated into the 1st and the 2nd reduction peaks, which were attributed to HNQ/HNQH (−320 mV), and HNQH/$HNQH_2$ (−650 mV), respectively, in Phase 4 (Fig. 7a). EIS was carried out at the first redox peak (−320 mV vs. Ag/AgCl). Fig. 7b shows the Nyquist plots of each phase. With MES-HNQ, the ohmic resistance (R_Ω) was approximately 1.5 Ω, and the charge transfer resistance showed a gradual decrease from 7.9 to 0.9 Ω (Table 1). The estimated R_{diff}s were approximately 10 Ω in all phases based on the circuit model (Fig. 3e).

3.4. Microbial communities by next-generation sequencing

At the end of Phase 4, the bacterial communities of planktonic cell and biofilm were characterized by next-generation sequencing (NGS) (Fig. 8 and Fig. S2). Fig. S2 shows the relative abundance of the species in OC, MES, MES-NR, and MES-HNQ compared to that of the initial inoculum. At the phylum level, Firmicutes increased from 5.4% (inoculum) to 43.3% in the biofilm of MES-HNQ. Similarly, Proteobacteria increased from 11.6 % to 70.8% in the biofilm of the MES-NR. In contrast, the relative abundance of Bacteroidetes decreased from 44.6% to 9.2% in the biofilm of MES-NR and MES-HNQ.

The major strains from different MES conditions were classified into Firmicutes, Proteobacteria, and Bacteroidetes, as shown in Fig. 8. The Firmicutes phylum consists of *Sporomusa*, *Clostridium*, and *Acetobacterium*, which are known as electrosynthesis-related strains [49]. Some of

Table 1
Acetate production from CO_2 electrosynthesis in MES.

Strain	Electrode Type	Potential (V)	volume (batch)	Acetate production		CE (%)	Ref.
				Rate (g/L/d)	Titer (g/L)		
Pure culture							
Sporomusa sphaeriodes	Graphite stick	−0.4	0.2L	0.002		84 ± 26 %	Nevin et al. (2011) [57]
Clostridium ljungdhalii	Graphite stick	−0.4	0.2L	0.003		88 ± 2 %	
Sporomusa ovata	Ni-coated graphite stick	−0.6	0.2L	3.4		84 %	Nie et al. (2013) [58]
Sporomusa ovata	Graphite stick	−0.74	0.L	0.315		105 ± 5 %	Giddings et al. (2015) [59]
Clostridium ljungdahlii	Graphite stick and felt	−0.9 to −1	0.3L (continuous; 3.3d HRT)	0.248	10.0	97 %	Bajracharya et al. (2017) [37]
Mixed culture							
Mix of anaerobic digester and retention basin effluents	Graphite granules	−0.6	0.45	0.024		28 ± 6.1 %	Batlle-Vilanova et al. (2016) [60]
Mix of secondly anaerobic digester effluents	Graphite felt	−1.1	0.325	0.561	4.5	82 %	Im et al. (2016) [61]
Enriched culture	Carbon felt	−1 ± 0.06	0.3	0.940	5.7	63 %	Arends et al. (2017) [62]
Mixed culture	Carbon felt	−0.85	0.094	9.85	8.6	87 %	Jourdin et al. (2018) [18]
Electroactive microbiome by Clostridium spp.	Graphite granules	−0.8 to −0.9	0.1	–	12.9		Vassilev et al. (2019) [63]
Anaerobic sludge	Carbon felt	2.6–2.8	0.625	–	5	95–97%	Vidales et al. (2021) [64]
Mix of secondly anaerobic digester effluents	Carbon felt	−1.11	0.25	0.276 0.44	8.26 (NR) 13.3 (HNQ)	87 % 92 %	This study

Table 2
Calculation of the EIS impedance by model fitting in OC, MES, MES-NR, and MES-HNQ. (Unit: Ω).

		AbioticControl	Inoculation	Phase 1	Phase 2	Phase 3	Phase 4
OC	R_{Ω}	0.4	0.2	0.3	0.4	0.4	0.4
	R_{ct}	10.1	20.5	18.7	84.1	341.5	953.3
	R_{diff}	574.9	59.4	104.9	168.6	–	–
MES	R_{Ω}	0.4	0.4	0.4	0.5	0.5	0.6
	R_{ct}	16.8	19.5	5.9	5.6	4.5	
	R_{diff}	53.6	529.5	21.7	17.8	11.2	10.1
MES-NR	R_{Ω}	0.3	0.3	0.4	0.5	0.7	0.7
	R_{ct}	15.2	13.5	5.6	6.9	4.6	3.5
	R_{diff}	2.0	2.1	7.8	7.5	8.2	7.7
MES-HNQ	R_{Ω}	0.3	0.4	0.3	0.5	0.6	0.7
	R_{ct}	7.9	7.9	2.6	1.5	0.9	0.9
	R_{diff}	–	–	11.5	11.2	11.3	10.7

* Ohmic resistance (R_{Ω}) from zero to start point of the first semicircle
* Charge transfer resistance (R_{ct}) estimated from the first semicircle at high frequency
* Diffusion resistance (R_{diff}) estimated from the second semicircle at low frequency

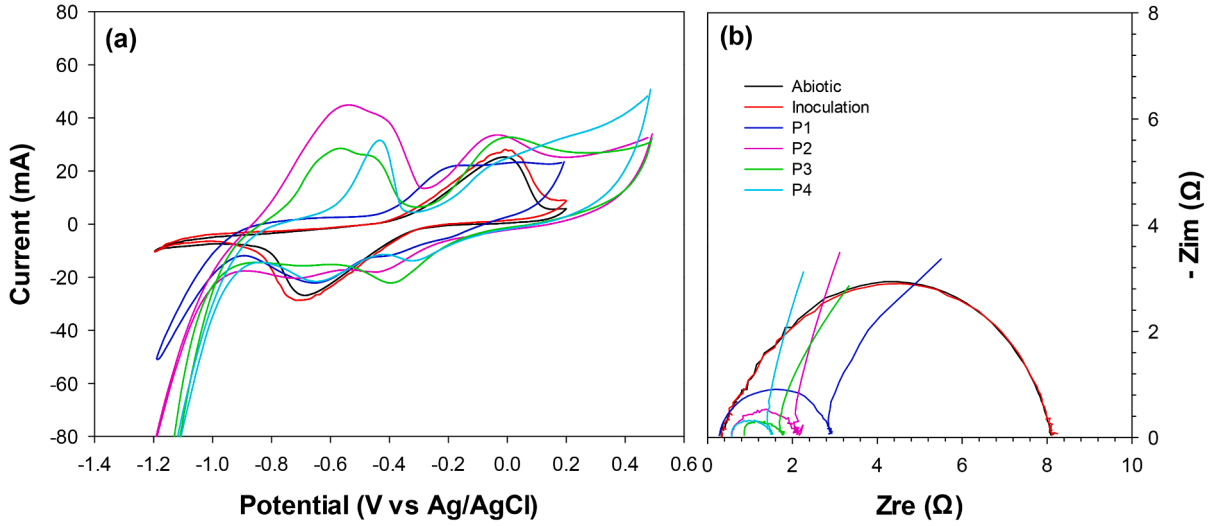

Fig. 7. Cyclic voltammetry (CV) and electrochemical impedance spectroscopy (EIS) of MES-HNQ. CV and EIS were carried out in the middle of each phase. (a) CV and (b) EIS.

the species occupied dominant abundance in each genus level in the classified OTU by partial sequencing. *Spromusa* is a primary acetogenic species that is the dominant genus in both biofilm and planktonic cells in MES-HNQ, whereas it is only dominant in the biofilm of MES [50]. *Spromusa sphaeroides* accounted for 16.5% of the electrosynthetic biofilm but only 1.5% of planktonic cells in MES. In MES-HNQ, *Spromusa sphaeroides* was highly populated in the biofilm (35.3%) and planktonic cells (22.1%). *Acetobacterium wieringae* was also reported as acetogenic species in electrosynthesis [51]. The relative abundance in MES-NR was 15.8% in the planktonic cells but only 3.0 % in the biofilm. Nevertheless, acetate production was higher in MES-NR (137.5 mM). These results suggest that such acetogen is involved in CO_2 electrosynthesis in planktonic cells instead of the biofilm with NR-supplemented conditions.

On the other hand, *Arcobacter, Pseudomonas*, and *Azonexus* were the major species in Proteobacteria. *Arcobacter* sp. was reported to produce ammonia or nitrate from nitrogen fixation under anaerobic conditions but could consume acetate as a carbon source [52]. Interestingly, *Arcobacter butzleri* accounted for 19.1 % and 16.8 % in the planktonic cells and biofilm of MES-NR, respectively, and approximately 10 % in the other MESs. *Pseudomonas caeni* is abundant in MES-HNQ with 31.0 % of planktonic cells and 19.3 % of the biofilm. *Azonexus* sp. reduces nitrate and nitrite to nitrogen and uses various organic acids as the carbon source [53]. *Azonexus caeni* was highly populated in planktonic cells (29.5–46.4 %) and in biofilms (18.1–25.1 %) from OC, MES, and MES-NR, but its level was negligible in the MES-HNQ. Therefore, MES-HNQ accumulates high acetate concentrations, whereas other MES lost acetate by acetate-consuming species, such as *Arcobacter* and *Azonexus*.

3.5. Taxonomic distribution and schematic diagram of bacterial community

The taxonomic distribution of communities of different MES was examined by principal coordinate analysis (PCoA) performed in QIIME (Fig. S3). The PCoA based on weighted UniFrac distances for all samples (n = 5) revealed four distinct clusters. Each cluster contained samples from each treatment. Interestingly, the average weighted UniFrac distances showed a significant difference between with and without a mediator in both the planktonic and biofilm environments (Fig. S3b and d). The microbial communities cluster of MES and OC showed closer UniFrac distances in planktonic and biofilm environments. In contrast, MES-NR and HNQ were relatively far away from that of MES without a mediator. The two mediators may induce different developments of the bacterial community and distribution in MES.

Fig. 9 presents a schematic diagram of the community interactions based on the major microbial taxonomic classification and phylum level

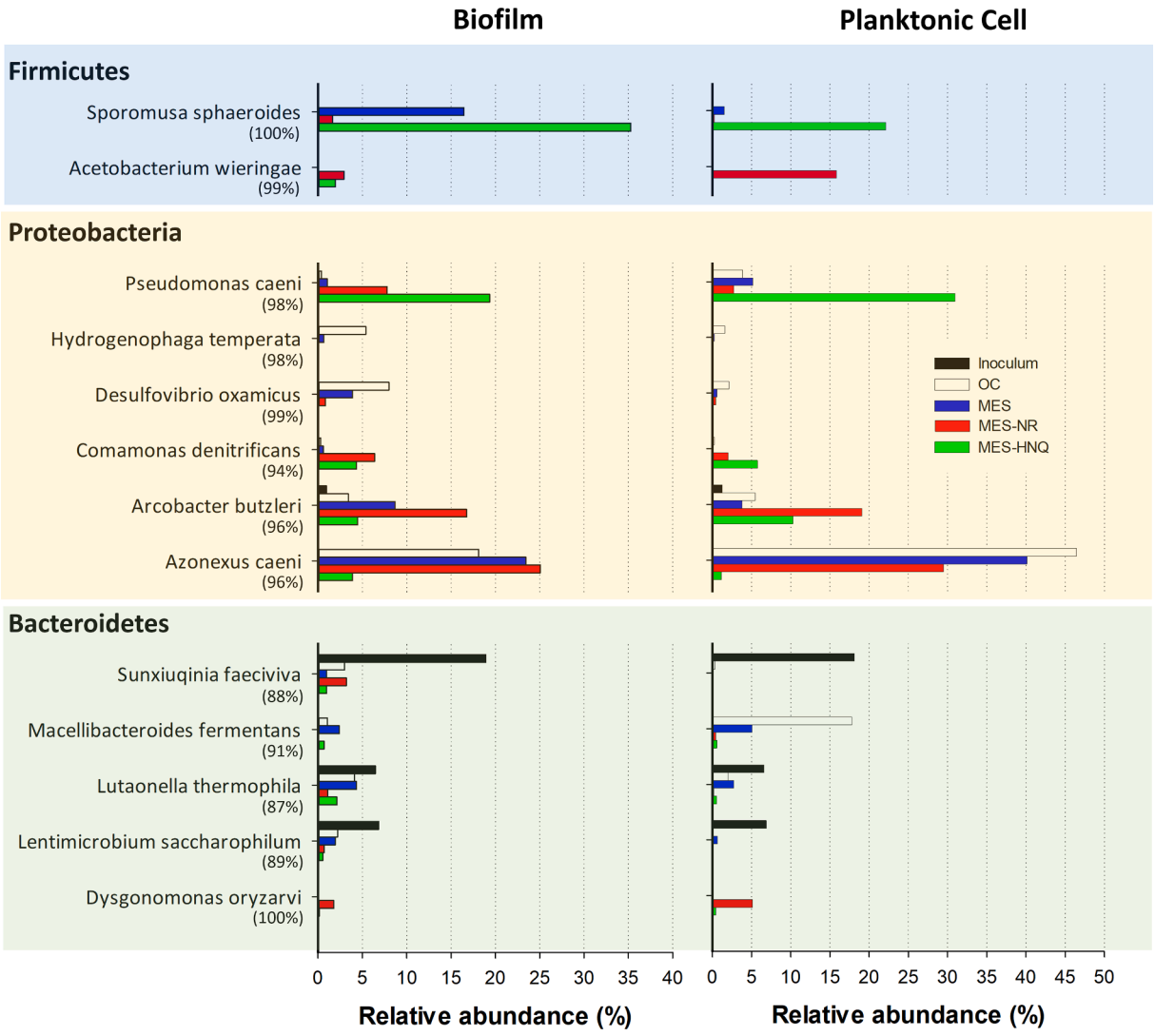

Fig. 8. Relative abundance of the microbial community profile of the major strains in the biofilm and planktonic cells at the species level.

analysis. Without artificial mediators, the unidentified self-producing shuttle molecules, such as pyocyanin and abiotically produced hydrogen molecules, may carry electrons to planktonic cells (Fig. 9a). In contrast, NR and HNQ act as efficient electron shuttles between the electrode and acetogenic species, such as *Acetobacterium* (in suspension) and *Sporomusa* (both suspension and biofilm). These results suggest that the electron mediator and regular media replacement poised selective pressure of the community in both suspension and biofilm on the electrode of MES.

4. Implication

Hydrogen is a common shuttle molecule in interspecies electron transfer in nature and microbial electrosynthesis. For the reducing equivalent of CO_2 reduction, hydrogen can be provided by an external supply or internal generation from an electrochemical reaction. The hydrogen can be produced easily at potentials lower than −420 mV vs. SHE (i.e., −630 mV vs. Ag/AgCl) at the cathode electrode by proton reduction. This potential is generally applied to the cathode in an MES reactor; thus, hydrogen is involved in most microbial CO_2 electrosynthesis processes. On the other hand, hydrogen is expensive to produce, meaning that the commercial feasibility of H_2-based electrosynthesis might be uncompetitive. The solubility of hydrogen is only 1.62 mg H_2/kg water at room temperature and pressure. Even when hydrogen is provided to the MES system, the microbial catalysts in the aqueous phase may not be able to utilize hydrogen as an electron shuttle/donor efficiently. In the perspective of reactor operation, the feed hydrogen can easily be lost without providing a reducing equivalent to the bioconversion.

In contrast, HNQ and NR deliver respiratory electrons efficiently to the cell through the aqueous phase and cell membranes. Although some mediators are toxic to cells, most are biocompatible. The menaquinone and quinone derivative shuttles can exchange electrons with enzymes and cofactors within the cell, such as NADH dehydrogenase and NAD^+/NADH [40,54] (Fig. S4). The use of shuttle molecules could overcome the intrinsic limitations of the electrode surface area, which expands the production capability into volumetric space in an electrode-based bioconversion reactor [43,55,56]. Nevertheless, it may have drawbacks with respect to the continuous operation and potential toxicity to the environment. On the other hand, NR and HNQ enrich the electrosynthetic biofilms and species under periodic media replacement and may provide a strategy for the stable operation of MES. Further study will be needed to develop control strategies for the bacterial community in biofilm and planktonic space and typical operational parameters of MES.

Supplementary Information Table S1 provides a preliminary estimation of the acetate production cost based on electrical energy. One kilogram of acetate production in the MES reactor consumed $2.57

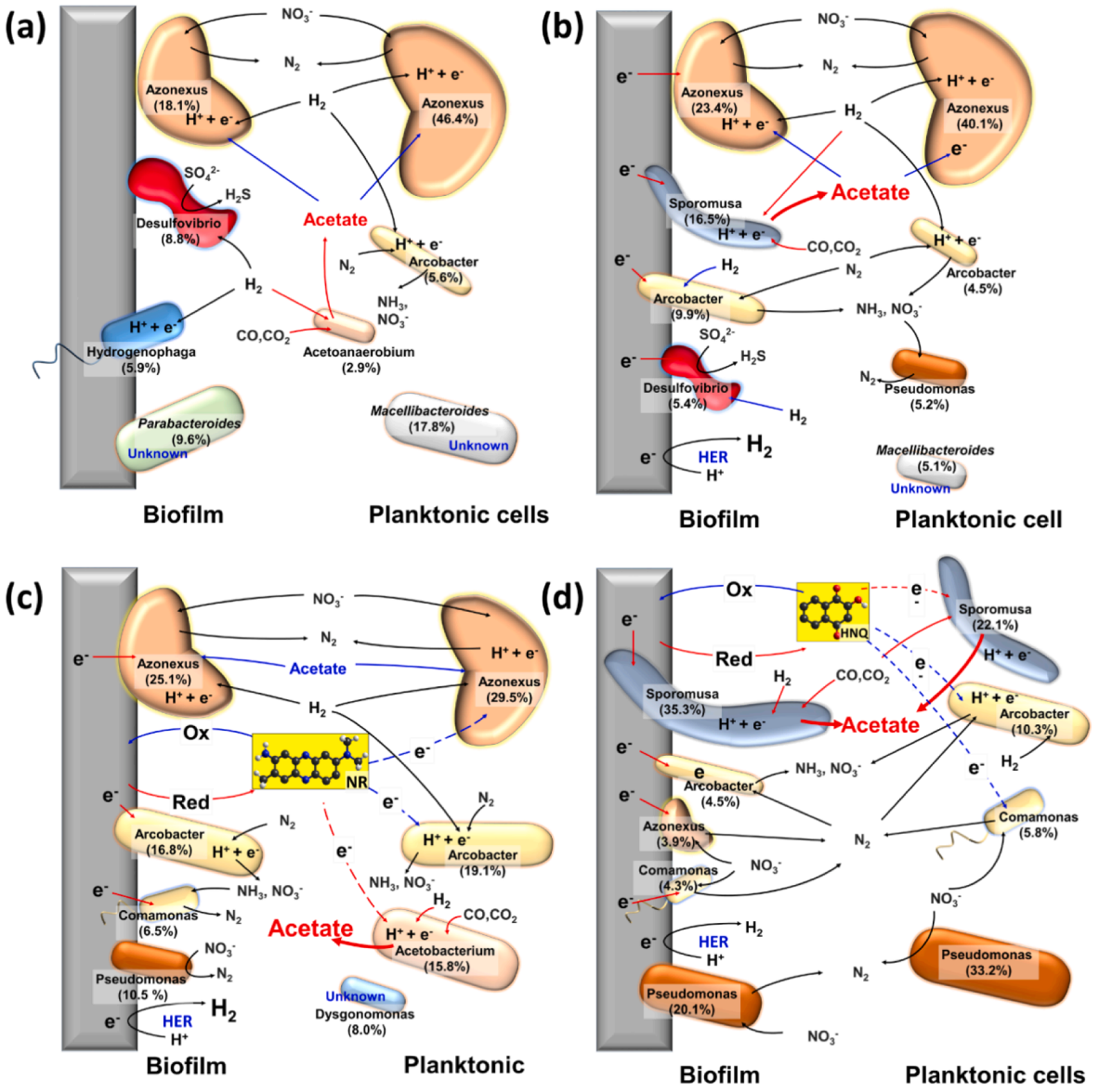

Fig. 9. Schematic diagram of the microbial community model of the interaction between a biofilm and planktonic cells. (a) OC, (b) MES, (c) MES-NR, and (d) MES-HNQ. Red arrow: acetate production, blue arrow: acetate consumption, black arrow: metabolic connection regardless of acetate production, red dash arrow: electron transfer via mediator for acetate production, blue dash arrow: electron transfer via mediator not related to acetate production. (For interpretation of the references to color in this figure legend, the reader is referred to the web version of this article.)

(MES), $1.15 (MES-NR), and $1.76 (MES-HNQ) of electrical energy. These are comparable with the current market price for acetate production ($0.77 per kilogram acetate). Nevertheless, additional estimations of the capital cost of reactor and operations other than electrical energy are needed. It is expected that the further optimization and scaled-up process reduce the cost of acetate production using MES.

5. Conclusion

Microbial electrosynthesis (MES) has been highlighted to valorize CO_2 into useful metabolites using electricity as the reducing power. This study examined the effects of an artificial mediator on the biofilm matrix and bacterial community development in MES. NR and HNQ increase the acetate synthesis level significantly to 13.3 ± 0.2 g/L in Phase 4. Media replacement also improved acetate production in MES with NR and HNQ (4.6 ± 0.4 vs. 7.4 ± 0.4 mmol/l/day, respectively) but deteriorated acetate production significantly in MES without such a mediator. CLSM showed that the biofilm matrix consisted of live and dead cells while the composition was different in MES with and without a mediator. The next-generation sequencing (NGS) showed that the acetogenic species of *Sporomusa* and *Acetobacterium* are the dominant species in MES with a mediator. These results showed that an electroactive shuttle molecule facilitates electron transfer between the electrode and the planktonic cells and biofilm matrix to improve the conversion of CO_2 to acetate.

Declaration of Competing Interest

The authors declare that they have no known competing financial interests or personal relationships that could have appeared to influence the work reported in this paper.

Acknowledgments

This study was supported by the Mid-Career Researcher Program (No. NRF-2021R1A2C2007841) through the National Research

Foundation of Korea (NRF), funded by the Ministry of Science, ICT & Future Planning of Korea (Prof. Jung Rae Kim) and the US National Science Foundation Award CBET #1706889 (Prof. Haluk Beyenal).

Appendix A. Supplementary data

Supplementary data to this article can be found online at https://doi.org/10.1016/j.cej.2021.131885.

References

[1] BP, BP Statistical Review of World Energy 2020, https://www.bp.com/content/dam/bp/business-sites/en/global/corporate/pdfs/energy-economics/statistical-review/bp-stats-review-2020-full-report.pdf, 2020.
[2] F. Gong, H. Zhu, Y. Zhang, Y. Li, Biological carbon fixation: From natural to synthetic, J. CO2 Util. 28 (2018) 221–227.
[3] F. Gong, Y. Li, Fixing carbon, unnaturally, Science 354 (2016) 830–831.
[4] S. Hernández, M.A. Farkhondehfal, F. Sastre, M. Makkee, G. Saracco, N. Russo, Syngas production from electrochemical reduction of CO 2: current status and prospective implementation, Green Chem. 19 (2017) 2326–2346.
[5] Y.E. Song, C. Kim, S. Li, J. Baek, E. Seol, C. Park, J.-G. Na, J. Lee, Y.-K. Oh, J. R. Kim, Supply of proton enhances CO electrosynthesis for acetate and volatile fatty acid productions, Bioresour. Technol. 320 (2021) 124245.
[6] S. Li, Y.E. Song, J. Baek, H.S. Im, M. Sakuntala, M. Kim, C. Park, B. Min, J.R. Kim, Bioelectrosynthetic conversion of CO2 using different redox mediators: electron and carbon balances in a bioelectrochemical system, Energies 13 (2020) 2572.
[7] M. del Pilar Anzola Rojas, R. Mateos, A. Sotres, M. Zaiat, E.R. Gonzalez, A. Escapa, H. De Wever, D. Pant, Microbial electrosynthesis (MES) from CO2 is resilient to fluctuations in renewable energy supply, Energy Convers. Manage. 177 (2018) 272–279.
[8] A. Prévoteau, J.M. Carvajal-Arroyo, R. Ganigué, K. Rabaey, Microbial electrosynthesis from CO2: forever a promise? Curr. Opin. Biotechnol. 62 (2020) 48–57.
[9] C. Koch, A. Kuchenbuch, F. Kracke, P.V. Bernhardt, J. Krömer, F. Harnisch, Predicting and experimental evaluating bio-electrochemical synthesis—a case study with clostridium kluyveri, Bioelectrochemistry 118 (2017) 114–122.
[10] E.V. LaBelle, C.W. Marshall, H.D. May, Microbiome for the electrosynthesis of chemicals from carbon dioxide, Acc. Chem. Res. 53 (2020) 62–71.
[11] P. Izadi, J.-M. Fontmorin, B. Virdis, I.M. Head, E.H. Yu, The effect of the polarised cathode, formate and ethanol on chain elongation of acetate in microbial electrosynthesis, Appl. Energy 283 (2021) 116310.
[12] F. Aulenta, L. Catapano, L. Snip, M. Villano, M. Majone, Linking bacterial metabolism to graphite cathodes: electrochemical insights into the H2-producing capability of desulfovibrio sp, ChemSusChem 5 (2012) 1080–1085.
[13] R. Karthikeyan, R. Singh, A. Bose, Microbial electron uptake in microbial electrosynthesis: a mini-review. Journal of Industrial Microbiology and Biotechnology. 46. 2019. 1419-1426.
[14] X. Deng, N. Dohmae, K.H. Nealson, K. Hashimoto, A. Okamoto, Multi-heme cytochromes provide a pathway for survival in energy-limited environments, Science Advances 4 (2018) eaao5682.
[15] S. Yu, N.V. Myung, Recent advances in the direct electron transfer-enabled enzymatic fuel cells, Front. Chem. 8 (2021).
[16] K. Rabaey, R.A. Rozendal, Microbial electrosynthesis—revisiting the electrical route for microbial production, Nat. Rev. Microbiol. 8 (2010) 706.
[17] Y. Jiang, R.J. Zeng, Bidirectional extracellular electron transfers of electrode-biofilm: mechanism and application, Bioresour. Technol. 271 (2019) 439–448.
[18] L. Jourdin, S.M. Raes, C.J. Buisman, D.P. Strik, Critical biofilm growth throughout unmodified carbon felts allows continuous bioelectrochemical chain elongation from CO2 up to caproate at high current density, Front. Energy Res. 6 (2018) 7.
[19] N. Aryal, A. Halder, P.-L. Tremblay, Q. Chi, T. Zhang, Enhanced microbial electrosynthesis with three-dimensional graphene functionalized cathodes fabricated via solvothermal synthesis, Electrochim. Acta 217 (2016) 117–122.
[20] S.M. Strycharz, R.H. Glaven, M.V. Coppi, S.M. Gannon, L.A. Perpetua, A. Liu, K. P. Nevin, D.R. Lovley, Gene expression and deletion analysis of mechanisms for electron transfer from electrodes to Geobacter sulfurreducens, Bioelectrochemistry 80 (2011) 142–150.
[21] F. Geppert, D. Liu, M. van Eerten-Jansen, E. Weidner, C. Buisman, A. ter Heijne, Bioelectrochemical power-to-gas: state of the art and future perspectives, Trends Biotechnol. 34 (2016) 879–894.
[22] D.R. Lovley, Powering microbes with electricity: direct electron transfer from electrodes to microbes, Environ. Microbiol. Rep. 3 (2011) 27–35.
[23] L. Jourdin, T. Grieger, J. Monetti, V. Flexer, S. Freguia, Y. Lu, J. Chen, M. Romano, G.G. Wallace, J. Keller, High acetic acid production rate obtained by microbial electrosynthesis from carbon dioxide, Environ. Sci. Technol. 49 (2015) 13566–13574.
[24] L. Chen, P.-L. Tremblay, S. Mohanty, K. Xu, T. Zhang, Electrosynthesis of acetate from CO 2 by a highly structured biofilm assembled with reduced graphene oxide–tetraethylene pentamine, J. Mater. Chem. A 4 (2016) 8395–8401.
[25] A. Gomez Vidales, S. Omanovic, B. Tartakovsky, Combined energy storage and methane bioelectrosynthesis from carbon dioxide in a microbial electrosynthesis system, Bioresour. Technol. Rep. 8 (2019), 100302.
[26] L. Jourdin, S. Freguia, V. Flexer, J. Keller, Bringing high-rate, CO2-based microbial electrosynthesis closer to practical implementation through improved electrode design and operating conditions, Environ. Sci. Technol. 50 (2016) 1982–1989.
[27] M.F. Alqahtani, K.P. Katuri, S. Bajracharya, Y. Yu, Z. Lai, P.E. Saikaly, Porous hollow fiber nickel electrodes for effective supply and reduction of carbon dioxide to methane through microbial electrosynthesis, Adv. Funct. Mater. 28 (2018) 1804860.
[28] B. Bian, J. Xu, K.P. Katuri, P.E. Saikaly, Resistance assessment of microbial electrosynthesis for biochemical production to changes in delivery methods and CO2 flow rates, Bioresour. Technol. 319 (2021), 124177.
[29] P.-L. Tremblay, L.T. Angenent, T. Zhang, Extracellular electron uptake: among autotrophs and mediated by surfaces, Trend. Biotechnol. 35 (2017) 360–371.
[30] H.D. May, P.J. Evans, E.V. LaBelle, The bioelectrosynthesis of acetate, Curr. Opin. Biotechnol. 42 (2016) 225–233.
[31] H. Seelajaroen, M. Haberbauer, C. Hemmelmair, A. Aljabour, L.M. Dumitru, A. W. Hassel, N.S. Sariciftci, Enhanced bio-electrochemical reduction of carbon dioxide by using neutral red as a redox mediator, ChemBioChem 20 (2019) 1196–1205.
[32] S. Bajracharya, K. Vanbroekhoven, C.J. Buisman, D.P. Strik, D. Pant, Bioelectrochemical conversion of CO2 to chemicals: CO2 as a next generation feedstock for electricity-driven bioproduction in batch and continuous modes, Faraday Discuss. 202 (2017) 433–449.
[33] L. Jourdin, T. Burdyny, Microbial electrosynthesis: where do we go from here? Trend. Biotechnol. 39 (2021) 359–369.
[34] F. Kracke, A.B. Wong, K. Maegaard, J.S. Deutzmann, M.A. Hubert, C. Hahn, T. F. Jaramillo, A.M. Spormann, Robust and biocompatible catalysts for efficient hydrogen-driven microbial electrosynthesis, Communications Chemistry 2 (2019) 45.
[35] J. Phillips, K. Klasson, E. Clausen, J. Gaddy, Biological production of ethanol from coal synthesis gas, Appl. Biochem. Biotechnol. 39 (1993) 559–571.
[36] J.B. Rollefson, C.E. Levar, D.R. Bond, Identification of genes involved in biofilm formation and respiration via mini-himar transposon mutagenesis of geobacter sulfurreducens, J. Bacteriol. 191 (2009) 4207–4217.
[37] S. Bajracharya, R. Yuliasni, K. Vanbroekhoven, C.J. Buisman, D.P. Strik, D. Pant, Long-term operation of microbial electrosynthesis cell reducing CO2 to multi-carbon chemicals with a mixed culture avoiding methanogenesis, Bioelectrochemistry 113 (2017) 26–34.
[38] O. Choi, B.-I. Sang, Extracellular electron transfer from cathode to microbes: application for biofuel production, Biotechnol. Biofuels 9 (2016) 1–14.
[39] A. Ter Heijne, O. Schaetzle, S. Gimenez, F. Fabregat-Santiago, J. Bisquert, D. P. Strik, F. Barrière, C.J. Buisman, H.V. Hamelers, Identifying charge and mass transfer resistances of an oxygen reducing biocathode, Energy Environ. Sci. 4 (2011) 5035.
[40] T.D. Harrington, V.N. Tran, A. Mohamed, R. Renslow, S. Biria, L. Orfe, D.R. Call, H. Beyenal, The mechanism of neutral red-mediated microbial electrosynthesis in escherichia coli: menaquinone reduction, Bioresour. Technol. 192 (2015) 689–695.
[41] D. Park, J. Zeikus, Utilization of electrically reduced neutral Red byactinobacillus succinogenes: physiological function of neutral Red in membrane-driven fumarate reduction and energy conservation, J. Bacteriol. 181 (1999) 2403–2410.
[42] D. Park, M. Laivenieks, M. Guettler, M. Jain, J. Zeikus, Microbial utilization of electrically reduced neutral red as the sole electron donor for growth and metabolite production, Appl. Environ. Microbiol. 65 (1999) 2912–2917.
[43] C. Kim, J.H. Lee, J. Baek, D.S. Kong, J.-G. Na, J. Lee, E. Sundstrom, S. Park, J. R. Kim, Small current but highly productive synthesis of 1,3-propanediol from glycerol by an electrode-driven metabolic shift in klebsiella pneumoniae L17, ChemSusChem 13 (2020) 564–573.
[44] H. Shin, J. Zeikus, M. Jain, Electrically enhanced ethanol fermentation by clostridium thermocellum and saccharomyces cerevisiae, Appl. Microbiol. Biotechnol. 58 (2002) 476–481.
[45] L. Girbal, I. Vasconcelos, S. Saint-Amans, P. Soucaille. How neutral red modified carbon and electron flow in Clostridium acetobutylicum grown in chemostat culture at neutral pH, FEMS microbiology reviews. 16. 1995. 151-162.
[46] C.H. Im, C. Kim, Y.E. Song, S.-E. Oh, B.-H. Jeon, J.R. Kim, Electrochemically enhanced microbial CO conversion to volatile fatty acids using neutral red as an electron mediator, Chemosphere 191 (2018) 166–173.
[47] A.K. Jordão, M.D. Vargas, A.C. Pinto, F.d.C. da Silva, V.F. Ferreira, Lawsone in organic synthesis, RSC Adv. 5 (2015) 67909–67943.
[48] Y.M. Hijji, B. Barare, Y. Zhang, Lawsone (2-hydroxy-1, 4-naphthoquinone) as a sensitive cyanide and acetate sensor, Sens. Actuators, B 169 (2012) 106–112.
[49] F. Kracke, I. Vassilev, J.O. Krömer, Microbial electron transport and energy conservation–the foundation for optimizing bioelectrochemical systems, Front. Microbiol. 6 (2015) 575.
[50] J. Philips, E. Monballyu, S. Georg, K. De Paepe, A. Prévoteau, K. Rabaey, J.B.A. Arends. An Acetobacterium strain isolated with metallic iron as electron donor enhances iron corrosion by a similar mechanism as Sporomusa sphaeroides. FEMS Microbiology Ecology. 95. 2018.
[51] M. Braun, G. Gottschalk. Acetobacterium wieringae sp. nov., a new species producing acetic acid from molecular hydrogen and carbon dioxide, Zentralblatt für Bakteriologie Mikrobiologie und Hygiene: I. Abt. Originale C: Allgemeine, angewandte und ökologische Mikrobiologie. 3. 1982. 368-376.
[52] I. Roalkvam, K. Drønen, R. Stokke, F.L. Daae, H. Dahle, I.H. Steen, Physiological and genomic characterization of arcobacter anaerophilus ir-1 reveals new metabolic features in epsilonproteobacteria, Front. Microbiol. 6 (2015) 987.
[53] Z.-X. Quan, W.-T. Im, S.-T. Lee, Azonexus caeni sp. nov., a denitrifying bacterium isolated from sludge of a wastewater treatment plant, Int. J. Syst. Evol. Microbiol. 56 (2006) 1043–1046.

[54] M. Boersch, S. Rudrawar, G. Grant, M. Zunk, Menaquinone biosynthesis inhibition: a review of advancements toward a new antibiotic mechanism, RSC Adv. 8 (2018) 5099–5105.
[55] C. Kim, M.Y. Kim, I. Michie, B.-H. Jeon, G.C. Premier, S. Park, J.R. Kim, Anodic electro-fermentation of 3-hydroxypropionic acid from glycerol by recombinant klebsiella pneumoniae L17 in a bioelectrochemical system, Biotechnol. Biofuels 10 (2017) 199.
[56] S. Mutyala, C. Kim, Y.E. Song, H. Khandelwal, J. Baek, E. Seol, Y.-K. Oh, J.R. Kim, Enabling anoxic acetate assimilation by electrode-driven respiration in the obligate aerobe Pseudomonas putida, Bioelectrochemistry 138 (2021), 107690.
[57] K.P. Nevin, S.A. Hensley, A.E. Franks, Z.M. Summers, J. Ou, T.L. Woodard, O. L. Snoeyenbos-West, D.R. Lovley, Electrosynthesis of organic compounds from carbon dioxide is catalyzed by a diversity of acetogenic microorganisms, Appl. Environ. Microbiol. 77 (2011) 2882–2886.
[58] H. Nie, T. Zhang, M. Cui, H. Lu, D.R. Lovley, T.P. Russell, Improved cathode for high efficient microbial-catalyzed reduction in microbial electrosynthesis cells, PCCP 15 (2013) 14290.
[59] C.G. Giddings, K.P. Nevin, T. Woodward, D.R. Lovley, C.S. Butler, Simplifying microbial electrosynthesis reactor design, Front. Microbiol. 6 (2015) 468.
[60] P. Batlle-Vilanova, S. Puig, R. Gonzalez-Olmos, M.D. Balaguer, J. Colprim, Continuous acetate production through microbial electrosynthesis from CO2 with microbial mixed culture, J. Chem. Technol. Biotechnol. 91 (2016) 921–927.
[61] C.H. Im, Y.E. Song, B.-H. Jeon, J.R. Kim, Biologically activated graphite fiber electrode for autotrophic acetate production from CO2 in a bioelectrochemical system, Carbon letters 20 (2016) 76–80.
[62] J.B. Arends, S.A. Patil, H. Roume, K. Rabaey, Continuous long-term electricity-driven bioproduction of carboxylates and isopropanol from CO2 with a mixed microbial community, J. CO2 Util. 20 (2017) 141–149.
[63] I. Vassilev, F. Kracke, S. Freguia, J. Keller, J.O. Krömer, P. Ledezma, B. Virdis, Microbial electrosynthesis system with dual biocathode arrangement for simultaneous acetogenesis, solventogenesis and carbon chain elongation, Chem. Commun. 55 (2019) 4351–4354.
[64] A. Gomez Vidales, G. Bruant, S. Omanovic, B. Tartakovsky, Carbon dioxide conversion to C1–C2 compounds in a microbial electrosynthesis cell with in situ electrodeposition of nickel and iron, Electrochim. Acta 383 (2021), 138349.